Reprinted from: ATOMIC MASSES AND FUNDAMENTAL CONSTANTS, VOL. 5 (1976)
Edited by J.H. Sanders and A.H. Wapstra
Book available from Plenum Publishing Corporation
227 West 17th Street, New York, New York 10011

RYDBERG CONSTANT MEASUREMENT USING cw DYE LASER AND H* ATOMIC BEAM

R. L. Barger, T. C. English and J. B. West

National Bureau of Standards
Boulder, Colorado USA

We would like to describe a new experiment which we have in progress for obtaining a greatly improved value for the Rydberg.[1] The accuracy of measurements using classical techniques have been limited to about 2×10^{-7} by Doppler broadening and discharge effects. A recent improvement of accuracy to about 1×10^{-8} was obtained[2] by using a pulsed dye laser to obtain laser saturated-absorption of the Balmer α line in a hydrogen discharge, thereby eliminating Doppler broadening. We hope to achieve an accuracy between 1×10^{-9} and 1×10^{-10} through use of a recently developed extremely stable cw dye laser[3] to produce saturated absorption of the Balmer α line in an atomic beam of 2 s hydrogen atoms. Simultaneous excitation with RF[4] should yield a double-resonance linewidth of about 1 MHz. Use of an atomic beam should eliminate systematic errors due to collisional effects and extraneous electromagnetic fields such as are encountered in discharges. For measuring the Balmer α wavelength to obtain the Rydberg, we shall use the frequency-controlled Fabry-Perot interferometer which was used for the wavelength measurement of the 3.39 μ CH_4 line[5]. This 3.39 μ CH_4 line will be used as the length standard for the measurement.[4] We expect the accuracy of our wavelength measurement to be limited to a few $\times 10^{-10}$ by already investigated systematic errors inherant in our interferometer, mainly diffraction effects.

With the beam of $n = 2$, $^1S_{\frac{1}{2}}$ hydrogen atoms, the transitions available for observation are shown in Fig. 1. The approximate level splittings are indicated. Selection rules allow the six hyperfine components shown for the optical transition, which has saturated absorption linewidth of about 30 MHz corresponding to

the 3P lifetime. Thus the four transitions $2^2S_{\frac{1}{2}}(F=1)$ to $3^2P_{\frac{1}{2}}(F=0,1)$ and to $3^2P_{3/2}(F=0,1)$ form overlapping doublets, but the two transitions $2^2S_{\frac{1}{2}}(F=0)$ to $3^2P_{\frac{1}{2}}(F=1)$ and to $3^2P_{3/2}(F=1)$ are well isolated singlets. For these singlets, the addition of RF radiation to mix the 3S and 3P levels should result in sharp lines with a width of about 1 MHz for the four double resonance transitions. The sum frequencies $\nu_{opt} + \nu_{rf}$ give the two transition frequencies of the $2^2S_{\frac{1}{2}}(F=0) - 3^2S_{\frac{1}{2}}(F=0,1)$ doublet. Setting the laser and RF on the 1 MHz-wide peak to within only 1/20 of the line width corresponds to obtaining the transition frequency to a part in 10^{10}.

The experimental arrangement of the hydrogen beam apparatus is indicated in Fig. 2. Hydrogen atoms are produced with an RF discharge in a cell having a multi-channel slit. The atoms then pass through an electron excitation region to convert a few per cent to the $2^2S_{\frac{1}{2}}$ state. Downstream, the laser beam is crossed at right angle with the hydrogen beam and retroreflected to produce the optical saturated absorption peak. RF in the same region produces the narrow double resonance peak. The peak is detected by observation of the number of 2s hydrogen atoms remaining in the beam downstream from the optical-RF excitation region. At the detection region, the beam passes through a quenching electric field and the resulting Lyman α photons are detected with a solar blind photomultiplier. Modulating the laser frequency over the peak gives the first derivative signal used to servo the laser frequency to the center of the peak, with the RF frequency fixed. The predicted shot-noise limited signal-to-noise ratio at line center is about 10^3 in one second, corresponding to a pointing precision on the lines of approximately 2×10^{-12}. This is about 2 orders of magnitude better than the expected limit of accuracy for our interferometer.

The stabilized cw dye laser[3] has a frequency stability of about 6×10^{-13} for an integration time of 300 sec, better than the shot noise limit for the hydrogen beam discussed above. The Allan variance of the frequency noise is shown in Fig. 3**A**.The short term stability should allow observation of lines as narrow as a few kHz, and the long term stability indicates the measurement accuracy which can be achieved. Although such good stability is not needed for this Rydberg measurement, it will be useful in our other experiments[6] such as saturated absorption of a state-selected calcium beam.

The technique for stabilizing the dye laser is indicated in Fig. 4. We use a jet of cresyl-violet dye dissolved in ethylene glycol in order to obtain sufficient power at the Balmer α wavelength. Since cresyl-violet absorption is very low at the

Ar^+ laser wavelengths and high at 6000Å, we use the Ar^+ laser to pump an auxilliary untuned rhodamine 6G dyelaser, and use the resulting 6000Å output to pump the cresyl-violet. In this way we have obtained about 100 mW single mode at 6563Å. The dye laser wavelength is locked to the servo cavity fringe, and the length of the servo cavity is in turn stabilized to either the 3.39 μ fringe, for tunable stability, or to the Lyman α signal for locking to the Balmer α line. The entire dye laser is enclosed in a pressure box, to which the servo cavity is connected, to provide the capability of pressure scanning the stabilized wavelength. With the frequency locked to Balmer α , part of the dye laser output is passed through the interferometer for the wavelength measurement.

The flat-plate frequency-controlled interferometer is described elsewhere[5]. The systematic errors inherant in the interferometry should limit the accuracy of our Balmer α wavelength measurement. These errors together with their estimated accuracy limits are included in Table 1.

Table 1. Predicted accuracy limits, $\delta R/R$

Dye laser stability	6×10^{-13}
Hydrogen beam stability (shot noise limit)	2×10^{-12}
Interferometer systematic errors	$\sim 4 \times 10^{-10}$
1. Fringe pointing	10^{-10}
2. Diffraction correction	$\sim 4 \times 10^{-10}$
3. Alignment of laser beam and interferometer axis	10^{-10}
Uncertainty in fundamental constants $\left(\frac{m_e}{m_p}\right)$	2×10^{-10}

Also given in Table 1 is the main uncertainty in the Rydberg contributed by uncertainties in the fundamental constants. The theory[7], relating the measured transition energy to the Rydberg, involves functions of the fine structure constant and the ratio of the electron mass to the proton mass. All terms appear to be negligible to the order of accuracy of this experiment except the factor $(1 + \frac{m_e}{m_p})$ used in converting the Rydberg for hydrogen

to the Rydberg for infinite mass, R_∞. This factor contributes an uncertainty to R_∞ of about 2×10^{-10}, and is probably less than the systematic errors which will arise in the interferometery.

The present status of our experiment is as follows. The stabilized laser works satisfactorily at the Balmer α wavelength, having more than the required stability and power output. Also, the interferometer system is complete. The hydrogen atomic beam apparatus is constructed; however, on our first try we were unable to detect any metastable atoms. We are now in the process of trying to locate and correct the problem.

References

1. G. W. Series, Contemp. Phys. 14, 49 (1974).
2. T. W. Hansch, M. H. Nayfeh, S. A. Lee, S. M. Curry and I. S. Shahin, Phys. Rev. Lett. 32, 1336 (1974).
3. R. L. Barger, J. B. West and T. C. English, Appl. Phys. Lett. (July 1975).
4. D. E. Roberts and E. N. Fortson, Phys. Rev. Lett. 31, 1539 (1973).
5. R. L. Barger and J. L. Hall, Appl. Phys. Lett. 22, 196 (1973).
6. R. L. Barger, Laser Spectroscopy, Ed. by R. G. Brewer and A. Mooradian, Plenum Press, New York (1974).
7. J. D. Garcia and J. E. Mack, J. Opt. Soc. Am. 55, 654 (1965).

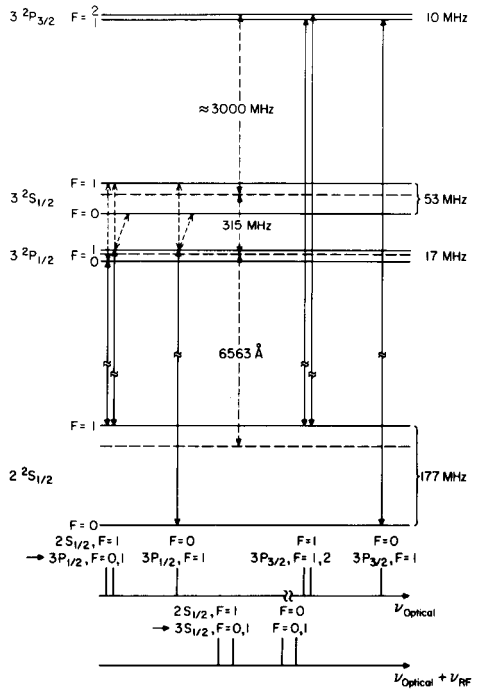

Fig. 1. Level diagram for the n=2→n=3 double resonance transition.

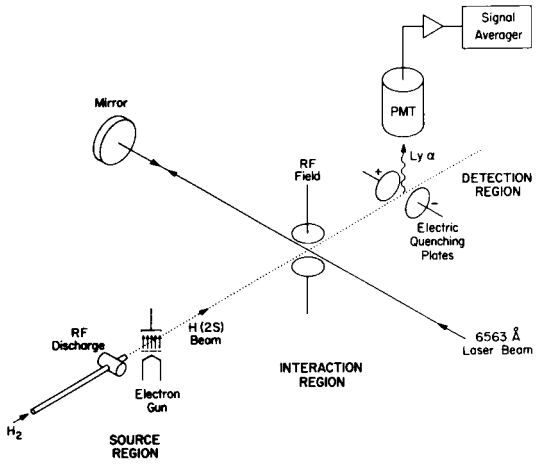

Fig. 2. Diagram of the hydrogen beam.

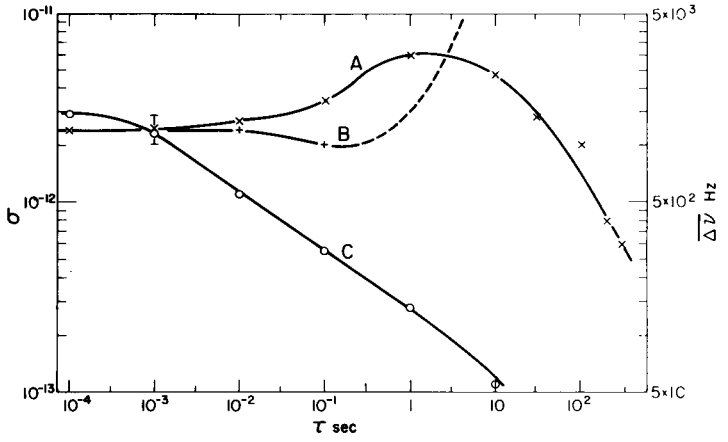

Fig. 3. Allan variance plot for cw dye laser, showing frequency stability vrs. integration time A.

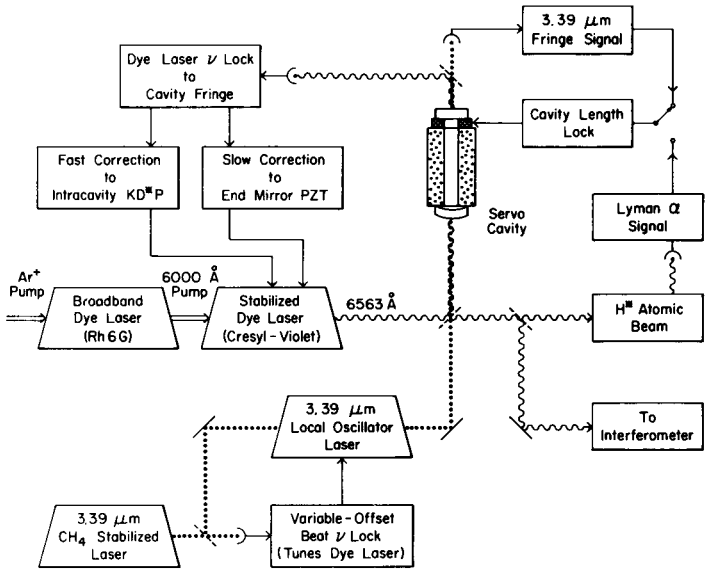

Fig. 4. Stabilization technique for cw dye laser.